

Boundary-Directed Epitaxy of Block Copolymers Toward Sub-10 nm Fabrication

To cite this article: Katherine Anna Su et al 2023 ECS Trans. 111 11

View the <u>article online</u> for updates and enhancements.

You may also like

 Integration of nanoimprint lithography with block copolymer directed self-assembly for fabrication of a sub-20 nm template for bitpatterned media

XiaoMin Yang, Shuaigang Xiao, Wei Hu et al.

- DIFFUSIVE SHOCK ACCELERATION AND RECONNECTION ACCELERATION PROCESSES

G. P. Zank, P. Hunana, P. Mostafavi et al.

 Electrocatalytic Aspects of the Chlorate Process: A Voltammetric and DEMS Comparison of RuO₂ and DSA Anodes Kateina Minhová Macounová, Nina Simic, Elisabet Ahlberg et al.



244th ECS Meeting

Gothenburg, Sweden • Oct 8 – 12, 2023

Early registration pricing ends September 11

Register and join us in advancing science!



Learn More & Register Now!

ECS Transactions, 111 (1) 11-16 (2023) 10.1149/11101.0011ecst ©The Electrochemical Society

Boundary-Directed Epitaxy of Block Copolymers Toward Sub-10 nm Fabrication

Katherine A. Su^a, Robert M. Jacobberger^a, Liliana Stan^b, and Michael S. Arnold^a

The directed self-assembly (DSA) of block copolymers (BCPs) can be used to produce nanoscale patterns without the cost and process complexity of state-of-the-art optical lithography. Thus, DSA may be useful in a wide variety of semiconductor applications such as fin field-effect transistors and biosensors. To create technologically useful patterns with aligned BCP domains, conventional DSA mechanisms often rely on topographically complex structures or high-resolution chemical patterns to direct the self-assembly, that are difficult to fabricate. In comparison, a newly discovered mechanism for DSA, termed boundary-directed epitaxy (BDE), utilizes chemical contrast at the boundaries between a substrate and relatively wide chemical stripe. Here, we demonstrate the use of BDE to template the fabrication of sub-10 nm features for the first time. BDE is used in conjunction with selective infiltration to create ultranarrow line-space arrays of alumina. These results demonstrate a proof-of-concept for BDE as a method for ultrahigh-resolution feature formation.

Introduction

Technology node scaling has historically been enabled by advances in optical lithography techniques that increase resolution (and thus decrease feature size). However, these techniques are often prohibitively expensive (as in extreme-UV lithography) (1) or complex to implement (as in multiple patterning techniques) (2, 3). Block copolymers (BCPs) are an attractive alternative considering their ability to self-assemble at the nanometer scale. When the molecular weight, volume fraction, interfacial energies, and block-to-block interaction parameters are carefully selected, a BCP can assemble into nanopatterns of alternating domains of vertical lamellae that are just a few nm thick. Directed self-assembly (DSA) can be used to position and orient these lamellae into patterns that are more technologically useful, such as lines, T-junctions, and jogs (3–6). However, conventional DSA mechanisms typically rely on either nm-scale resolution chemical patterns that are difficult to fabricate (chemoepitaxy) (3–5, 7) or topological features that complicate BCP deposition and can be difficult to remove (graphoepitaxy) (8, 9).

Here, we explore boundary-directed epitaxy, a newly discovered paradigm for DSA that utilizes the chemical contrast at the boundaries between a substrate and relatively wide chemical stripe to direct self-assembly (6). Notably, aligned and highly density-multiplied BCP nanopatterns with half-pitch of 6.8 nm are created using stripes

^a Department of Materials Science and Engineering, University of Wisconsin-Madison, Madison, Wisconsin 53706, USA

^b Center for Nanoscale Materials, Argonne National Laboratory, Lemont, Illinois 60439, USA

as wide as 100 nm. Then, these patterns are processed with sequential infiltration synthesis (SIS) and reactive-ion etching (RIE) to fabricate sub-10 nm alumina line-space arrays.

Results and Discussion

Stripes of monolayered graphene on Ge substrates are used to create the chemical contrast needed for boundary-directed epitaxy and for directing BCP assembly. The sharp chemical contrast at the boundaries of each graphene stripe is the driving force needed to orient and align the BCP domains. These boundaries are specifically fabricated via bottom-up chemical vapor deposition (CVD) of graphene stripes on Ge(001) as in (10). Ge(001) substrates are loaded into a CVD quartz tube furnace with an inner diameter of 34 mm. The system is evacuated to <10⁻³ Torr and then refilled to atmospheric pressure with a 1:2 mixture of H₂ in Ar. The samples are annealed for 1 hour at 910 °C to remove adventitious carbon that would otherwise nucleate graphene growth. Then, 4.6 sccm of CH₄ is introduced to initiate graphene growth. Growth is terminated by sliding the furnace away from the samples and stopping the CH₄ flow. This process results in stripes of graphene that are approximately 50-100 nm wide and 0.8-1 µm long with densities of approximately 2 per µm² (Figure 1a).

Poly(propylene carbonate)-block-poly(styrene)-block-poly(propylene carbonate) (PPC-b-PS-b-PPC) (from Polymer Source, Inc., $M_W \approx 5\text{-}10\text{-}5$ kg/mol) with a domain spacing (L_0) of 13.5 nm is then deposited onto the graphene-Ge templates via spin-coating from a 0.5 wt% solution in chlorobenzene, resulting in disordered BCP films with a thickness of $\sim L_0$ (Figure 1b). After spin-coating, the samples are annealed in an inert atmosphere at 160 °C for 10 min to allow the BCP domains to micro-segregate and self-assemble.

In the absence of chemical contrast boundaries, on bare graphene, the PPC-b-PS-b-PPC forms only horizontal lamellae with PS domains in contact with the graphene due to the preferentiality of the PS-graphene interface. Likewise, on bare Ge, the PPC-b-PS-b-PPC forms horizontal lamellae with PPC domains in contact with the Ge due to the preferentiality of the PPC-Ge interface. However, when pairs of closely spaced graphene-germanium boundaries are present, they sharply direct the lamellae orientation from horizontal to vertical in the region between the boundaries (Figure 1c). The vertical lamellae have widths of $\sim 0.5 L_0$ and can have a density multiplication as high as 6.5, depending on the width of the graphene stripe. Their long axes are aligned with the boundaries, enabling the patterning of lines, T-junctions, and jogs.

SIS, which entails sequential exposure to an organometallic Al₂O₃ precursor and H₂O, is used to grow AlO_x within the more polar PPC domain and fabricate alumina line-space arrays based on a procedure established in (11). SIS is performed at 90 °C with six 200 ms pulses of trimethylaluminum (TMA), a 400 s exposure, and a 300 s N₂ purge followed by six 200 ms pulses of H₂O, a 400 s exposure, and a 300 s N₂ purge. This selective infiltration is confirmed via increased SEM image contrast between the infiltrated PPC and the non-infiltrated PS vertical lamellae (Figure 2a). The presence of contrast on either side of the stripe, where there should be non-infiltrated PS horizontal

lamellae, indicates excess AlO_x deposition that may be reduced by decreasing the number of TMA pulses or TMA exposure time.

After SIS, O_2 RIE is performed on the samples. Due to the significant etch contrast between the non-infiltrated PS and AlO_x -infiltrated PPC, the PS is etched, leaving behind alumina line-space arrays where the line-widths are $\sim 0.5 L_0$. An SEM image, AFM topography map, and line profile of two different etched samples are shown in Figure 2b-c. The SEM image shows that the etching process does not remove the AlO_x domains. The AFM image and line profiles along the stripe width show that the PS lamellae etch much more quickly than the AlO_x , leaving behind AlO_x line-space arrays. The distances between the alumina lines are smaller than the AFM tip lateral resolution, so the absolute height numbers on the line profiles are not indicative of actual feature heights. The vertical lamellae also show dislocation and disinclination defects that may occur due to inhomogeneous graphene stripe width. The features observed on either side of the stripe likely originate from excess AlO_x growth during the SIS process.

Conclusion

In boundary-directed epitaxy, boundaries between surface regions of differing chemical composition direct BCP assembly into technologically useful patterns. We demonstrate here that these patterns can be used to fabricate sub-10 nm features through selective infiltration and etching. As it uses stripes that are both relatively wide and atomically thin, boundary-directed epitaxy addresses some of the challenges faced by previously established DSA methods. Ultimately, boundary-directed epitaxy is a promising alternative to conventional lithographic techniques.

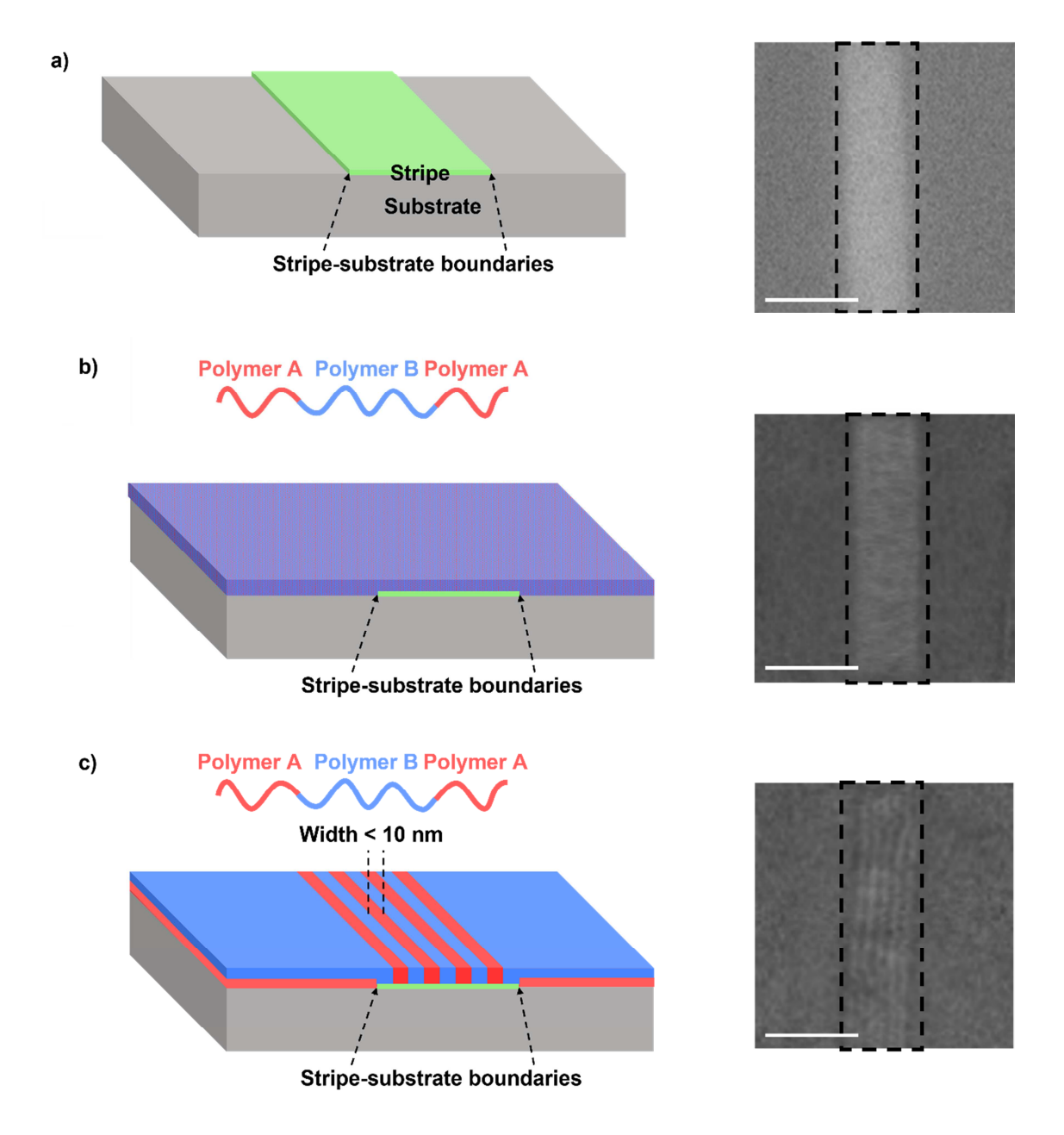


Figure 1. Schematics and SEM images of a) graphene stripes grown on Ge via CVD, b) a disordered BCP film after deposition via spin-coating on top of a graphene stripe, and c) vertical lamellae on top of a graphene stripe after assembly of the BCP via boundary-directed epitaxy. In all images, the location of the graphene stripe is outlined in black, and the scale bar is 100 nm.

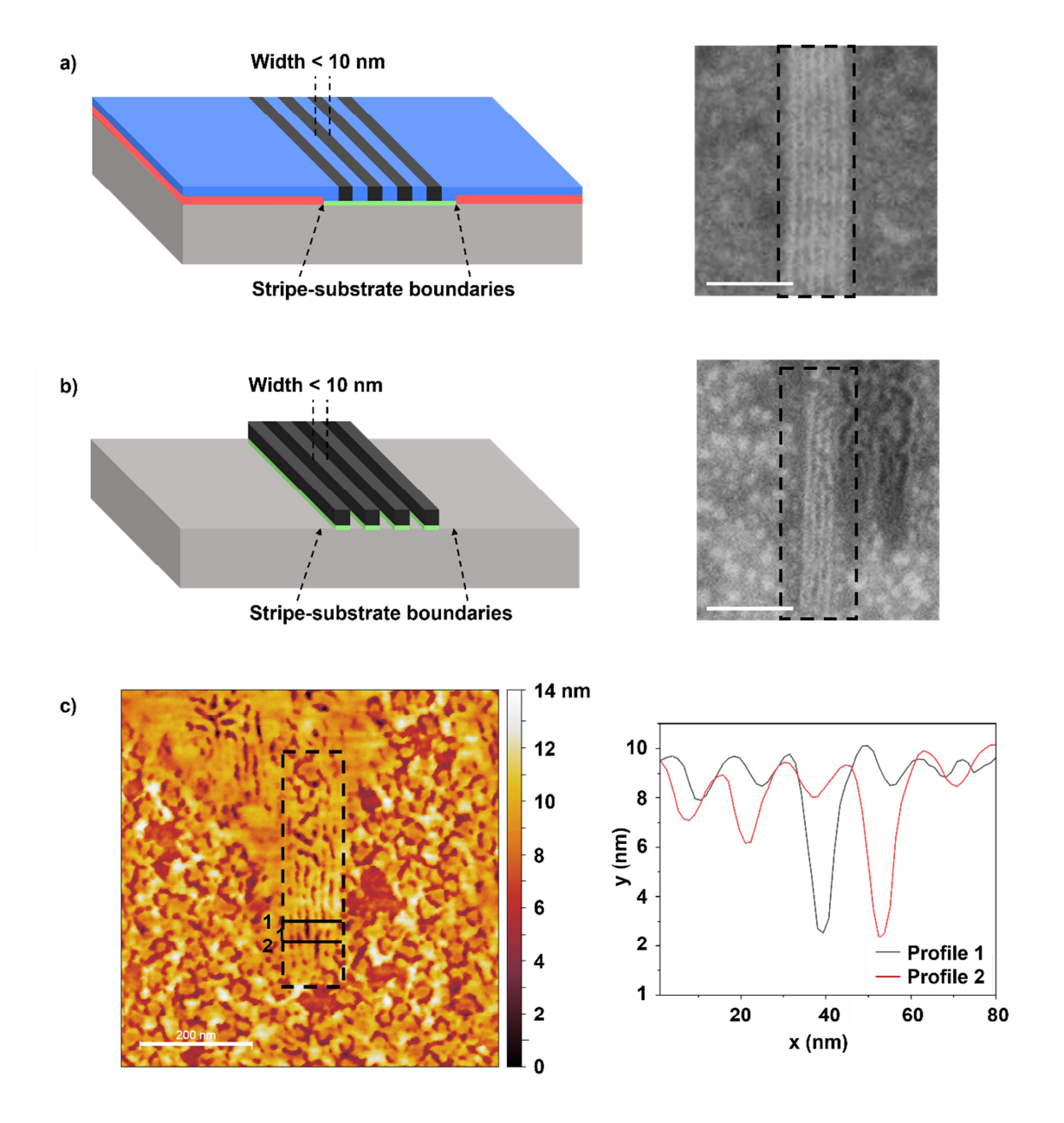


Figure 2. Fabrication of alumina line-space arrays. Schematics and SEM images of vertical lamellae on the graphene stripes after a) AlO_x infiltration via SIS and b) O_2 reactive-ion etching. c) AFM topography map and line profile of vertical lamellae after O_2 reactive-ion etching. The scale bars for a) and b) are 100 nm; the scale bar for c) is 200 nm.

Acknowledgments

This material is based upon work supported by the National Science Foundation under Grant No. 2011254 (K.A.S., M.S.A.). K.A.S. also acknowledges support from the National Science Foundation Graduate Research Fellowship under Grant No. DGE-1747503. Work performed at the Center for Nanoscale Materials, a U.S. Department of

Energy Office of Science User Facility, was supported by the U.S. DOE, Office of Basic Energy Sciences, under Contract No. DE-AC02-06CH11357. The authors gratefully acknowledge use of facilities and instrumentation at the UW-Madison Wisconsin Centers for Nanoscale Technology (wcnt.wisc.edu) partially supported by the National Science Foundation through the University of Wisconsin Materials Research Science and Engineering Center under Grant. No. DMR-1720415.

References

- 1. B. Wu and A. Kumar, *Appl. Phys. Rev.*, **1**, 011104 (2014).
- 2. D. C. Wack, J. Hench, L. Poslavsky, J. Fielden, V. Zhuang, W. Mieher, and T. Dziura, *Proc. SPIE*, **6922**, 602-610 (2008).
- 3. C.-C. Liu, E. Franke, Y. Mignot, R. Xie, C. W. Yeung, J. Zhang, C. Chi, C. Zhang, R. Farrell, K. Lai, H. Tsai, N. Felix, and D. Corliss, *Nat. Electron.*, 1, 562–569 (2018).
- 4. C.-C. Liu, A. Ramírez-Hernández, E. Han, G. S. W. Craig, Y. Tada, H. Yoshida, H. Kang, S. Ji, P. Gopalan, J. J. de Pablo, and P. F. Nealey, *Macromolecules*, **46**, 1415–1424 (2013).
- 5. E. W. Edwards, M. Müller, M. P. Stoykovich, H. H. Solak, J. J. de Pablo, and P. F. Nealey, *Macromolecules*, **40**, 90–96 (2007).
- 6. R. M. Jacobberger, V. Thapar, G.-P. Wu, T.-H. Chang, V. Saraswat, A. J. Way, K. R. Jinkins, Z. Ma, P. F. Nealey, S.-M. Hur, S. Xiong, and M. S. Arnold, *Nat. Commun.*, **11**, 4151 (2020).
- 7. C.-C. Liu, E. Han, M. S. Onses, C. J. Thode, S. Ji, P. Gopalan, and P. F. Nealey, *Macromolecules*, **44**, 1876–1885 (2011).
- 8. J. Doise, J. P. Bekaert, B. T. Chan, S. E. Hong, G. Lin, and R. Gronheid, *JM3.1*, **15**, 031603 (2016).
- 9. B. L. Peters, B. Rathsack, M. Somervell, T. Nakano, G. Schmid, and J. J. de Pablo, J. Polym. Sci., Part B: Polym. Phys., 53, 430–441 (2015).
- 10. R. M. Jacobberger, B. Kiraly, M. Fortin-Deschenes, P. L. Levesque, K. M. McElhinny, G. J. Brady, R. Rojas Delgado, S. Singha Roy, A. Mannix, M. G. Lagally, P. G. Evans, P. Desjardins, R. Martel, M. C. Hersam, N. P. Guisinger, and M. S. Arnold, *Nat. Commun.*, **6**, 8006 (2015).
- 11. T. Segal-Peretz, J. Winterstein, M. Doxastakis, A. Ramírez-Hernández, M. Biswas, J. Ren, H. S. Suh, S. B. Darling, J. A. Liddle, J. W. Elam, J. J. de Pablo, N. J. Zaluzec, and P. F. Nealey, *ACS Nano*, **9**, 5333–5347 (2015).